Wnt Modulators in the Aqueous Humor Are Associated With Outer Retinal Damage Severity in Patients With Neovascular Age-Related Macular Degeneration

Kyu Hyung Park,[1] Ae Jin Choi,[2] Jeehyun Yoon,[2] Daehan Lim,[2] Se Joon Woo,[1] Sang Jun Park,[1] Hyung Chan Kim,[2,3] and Hyewon Chung[2,3]

[1]Department of Ophthalmology, Seoul National University College of Medicine, Seoul National University Bundang Hospital, Seongnam, Korea
[2]Department of Ophthalmology, Konkuk University School of Medicine, Seoul, Korea
[3]Department of Ophthalmology, Konkuk University Medical Center, Seoul, Korea

Correspondence: Hyewon Chung, Department of Ophthalmology, Konkuk University School of Medicine, Konkuk University Medical Center, 120-1 Neungdong-ro, Gwangjin-gu, Seoul, Republic of Korea, 143-729; hchung@kuh.ac.kr.

Submitted: April 10, 2014
Accepted: July 3, 2014

Citation: Park KH, Choi AJ, Yoon J, et al. Wnt modulators in the aqueous humor are associated with outer retinal damage severity in patients with neovascular age-related macular degeneration. *Invest Ophthalmol Vis Sci*. 2014;55:5522–5530. DOI: 10.1167/iovs.14-14566

Purpose. To investigate the associations of the Wnt modulators Wnt inhibitory factor 1 (WIF-1) and Dickkopf 3 (DKK-3) in the aqueous humor with neovascular age-related macular degeneration (nAMD) and to determine their clinical implications.

Methods. Seventy-four nAMD patients initially treated with an intravitreal injection of ranibizumab (IVR) and 74 age- and sex-matched controls were studied. Aqueous humor WIF-1 and DKK-3 levels were measured by Western blotting and an ELISA before and 1 month after two consecutive IVRs (pre- and post-IVR). Visual acuity assessments and spectral domain optical coherence tomography were performed pre- and post-IVR.

Results. Western blotting showed increased WIF-1 and DKK-3 in 12 nAMD patients compared with 12 controls. The ELISA analysis demonstrated elevated WIF-1 (pre) and DKK-3 (pre) in 62 patients compared with 62 controls (54.7 vs. 23.0 and 114.3 vs. 93.0 ng/mL, respectively). In multivariate analyses, high WIF-1 (pre) levels were associated with increased disruption in the photoreceptor junction's inner and outer segments (IS/OS) (pre and post) and high WIF-1 (post) levels. Interestingly, WIF-1 (pre) levels were significantly higher in type 3 neovascularization (NV) patients than in type 1 or 2 NV (90.5 ± 36.7 vs. 48.3 ± 22.5 and 41.3 ± 28.8 ng/mL, respectively). However, choroidal thickness was not correlated with WIF-1 levels.

Conclusions. We report, for the first time, the possibility of phenotypic, anatomic, and ocular proteomic correlations, demonstrating correlated WIF-1 and DKK-3 upregulation in nAMD patients' aqueous humor. Secreted WIF-1, reflecting the degree of retinal structure damage, may be a new biomarker for the retina's healthy and disease states.

Keywords: age-related macular degeneration, Wnt, aqueous humor, optical coherence tomography, CNV

Age-related macular degeneration (AMD) is a disease of unknown etiology characterized by the progressive degeneration of the RPE, retina, and choriocapillaris and is the leading cause of blindness in people older than 50 years in developed countries. Extensive basic and clinical research, including studies of AMD risk genotypes,[1–4] has been performed to elucidate the causes of this disease. The associated underlying cellular pathologies suggested to date include oxidative stress, hypoxia, chronic inflammation, the accumulation of lipofuscin, and the accumulation of extracellular deposits, such as drusen. Functional abnormalities or the degeneration of the RPE are believed to be the initiators and major pathologies of AMD, and the pathogenic mechanistic studies of AMD conducted to date have primarily concentrated on RPE pathology. However, the response and pathology of the retina during AMD are largely unknown. Few studies have identified the molecular changes of the stressed retina in vivo. Proteins or cytokines in the aqueous humor (AH), such as VEGF, have been used as biomarkers of neovascular AMD (nAMD), neovascularization, and disease activity associated with AMD.[5,6] However, no proteins or cytokines that reflect the status or function of the retina and photoreceptors in this disease have been previously described in the AH of AMD patients.

The Wnt signaling pathways have been linked to various cellular processes, including inflammation, angiogenesis, and cell survival, development, and differentiation.[7–11] Recently, the Wnt pathway has been suggested to be a pathogenic mechanism of AMD, especially nAMD.[8] The therapeutic effects of Wnt inhibitors, such as monoclonal antibodies to Wnts, have been demonstrated in a mouse model of wet AMD.[8] However, others reported that increased Wnt signaling in light-induced retinal degeneration plays a role in retinal protection.[7,12] They suggested that upregulated Wnt signaling in Müller glia during retinal degeneration could be a protective mechanism to prevent further photoreceptor injury. These findings suggest that increased Wnt signaling could have different effects on the RPE, the retina, and neovascularization (NV), which is

consistent with other studies showing that the effect of Wnt signaling is cell- and tissue-dependent.[12]

In previous studies, we first identified Wnt modulator proteins, namely, Wnt inhibitory factor 1 (WIF-1) and Dickkopf 3 (DKK-3), in the AH and in AH exosomes in patients with nAMD.[13,14] The secreted frizzled-related protein family, the Dickkopf family, and WIF-1 have been identified as three classes of secreted antagonists of the Wnt pathway.[15–17] The DKK-3 was reported to exist in the inner nuclear and ganglion cell layers of the retina in normal and degenerating tissue and is expressed at high levels in rd1 animals.[18] The DKK-3 was suggested to be a secreted prosurvival signaling protein in the retina.[12]

The WIF-1, a secreted glycoprotein that inhibits the activity of Wnts, was first described in the retina by Hsieh and associates in 1999.[17] Although WIF-1 is reported to be located throughout the retina and is concentrated in the interphotoreceptor matrix, particularly in the region surrounding the inner segments and at the distal tips of the photoreceptors in adult mice,[19] the functional roles of WIF-1 in the retina remain poorly investigated. The expression of WIF-1 in the retina of AMD patients also has not been studied previously. During the past decade, WIF-1 has been studied in various cancers, including lung cancer, breast cancer, renal cancer, osteosarcoma, and acute myeloid leukemia.[20–24] The silencing of WIF-1 by DNA hypermethylation and subsequent Wnt activation has been implicated in the pathogenesis of these cancers.

Considering the known role of Wnt signaling in AMD, we speculate that the secreted Wnt modulators WIF-1 and DKK-3 may be dysregulated in AMD. In the present study, the AH levels of these proteins were examined in patients with nAMD who had received no previous treatment and in age- and sex-matched controls. In addition, their relationship to outer retinal morphology and the choroid was measured by spectral domain optical coherence tomography (SD-OCT), and the type of NV and its prognostic value in these patients were investigated.

Methods

Subjects and AH Sample Collection

Samples of AH were collected at the Department of Ophthalmology, Konkuk University Medical Center, Seoul, Korea, and the Department of Ophthalmology, Seoul National University Bundang Hospital, Seongnam, Korea. From July 1, 2012, to December 31, 2013, 74 patients with untreated nAMD and 74 age- and sex-matched controls undergoing cataract surgery were enrolled in this study. The 74 sets of patient samples consisted of samples from patients before the first intravitreal injection of 0.5 mg ranibizumab (IVR) and samples obtained from patients 1 month after two consecutive IVRs (pre- and post-IVR). The 74 patients were all untreated patients (i.e., they had not received any type of treatment for nAMD before their inclusion in the study). Eyes with massive subretinal hemorrhaging were excluded. In addition, these patients showed no manifestation of chronic nAMD, such as disciform scarring. Patients with ophthalmic diseases other than AMD (e.g., glaucoma or progressive retinal disease), patients with uncontrolled systemic diseases (e.g., uncontrolled diabetes mellitus or systemic hypertension), and patients who had undergone intraocular surgery, including laser treatment, were excluded. Samples of AH from patients undergoing cataract surgery were used as control samples. We matched the ages and sexes of the patients with those of the control subjects (±5 years). The control subjects did not have any ophthalmic disease other than cataracts. Control samples were obtained immediately before cataract surgery. Samples from nAMD patients were obtained before performing the first IVR and immediately before performing the third IVR. Twelve sets of samples (36 samples) were used as a discovery set for the Western blot analysis of WIF-1 and DKK-3, and 62 sets of samples were used for ELISA analysis as a validation set. The clinical data from 62 patients and 62 controls are summarized in Table 1.

Table 1. Baseline Characteristics of Patients With nAMD and Their Controls

	nAMD, $n = 62$	Controls, $n = 62$	*P* Value
Age, y (±SD)	70.9 (±6.7)	70.9 (±8.3)	0.9811*
Sex, male:female	31:31	31:31	1.0000†
Diabetes	10	12	0.4882†
Systemic hypertension	28	24	0.4666†
Smoking status			
Never	44	47	0.8036†
Quit	10	9	
Current	8	6	
NV type (1, 2, 3)			
1, sub-RPE (PCV)	41 (13)		
2, subretina	10		
3, RAP	11		
WIF-1 (pre), ng/mL	54.7 (±31.0)	23.0 (±10.5)	<0.0001*
DKK-3 (pre), ng/mL	114.3 (±46.8)	93.0 (±47.8)	0.0288*

nAMD, neovascular age-related macular degeneration; SD, standard deviation; NV, neovascularization; PCV, polypoidal choroidal vasculopathy; RAP, retinal angiomatous proliferation; WIF-1 (pre), level of Wnt inhibitory factor 1 before treatment with ranibizumab; DKK-3 (pre), level of Dickkopf 3 before treatment with ranibizumab.

* Student's *t*-test.

† Pearson's χ^2 test.

All sample collection and intravitreal injections were performed using standard sterile methods. Samples of AH were obtained by anterior-chamber paracentesis using a 30-gauge needle, with no complications. Samples of the AH (approximately 100 μL) in safe-lock microcentrifuge tubes (1.5 mL) were immediately frozen at −80°C and stored until analysis. The study followed the guidelines of the Declaration of Helsinki, and informed written consent was obtained from all patients and control subjects. The procedure for AH collection was approved by the institutional review boards of the Konkuk University Medical Center, Seoul, Korea, and the Seoul National University Bundang Hospital, Seongnam, Korea.

Western Blot Analysis of WIF-1 and DKK-3

The AH proteins were quantified using the BCA protein assay (Thermo Scientific, Waltham, MA, USA), and equivalent amounts of protein (10 μg) were applied to 12% acrylamide gels. The proteins were separated by SDS-PAGE and transferred to polyvinylidene fluoride (PVDF) membranes (Millipore, Billerica, MA, USA). The membranes were blocked at room temperature with 5% bovine serum albumin in TBST (1× Tris-buffered saline with 0.1% Tween 20) for 2 hours. The membranes were incubated with primary antibodies (WIF-1: Abcam, Cambridge, MA, USA; DKK-3: Thermo Scientific) overnight at 4°C. The membranes were then washed four times in TBST and incubated with the relevant horseradish peroxidase-conjugated secondary antibodies (Cell Signaling, Beverly, MA, USA) for 1 hour. After washing four times in TBST, immunoreactive proteins were visualized using a chemiluminescent substrate (ECL Prime; Amersham Biosciences, Piscataway, NJ, USA). The Luminescent Image Analyzer LAS-4000

with Image Reader LAS-4000 software (Fuji Film Co., Ltd., Tokyo, Japan) was used as a digital imaging system.

Measurement of WIF-1 and DKK-3 Using ELISA

The levels of WIF-1 and DKK-3 in the AH were quantitatively assessed using a sandwich ELISA kit (Aviscera Bioscience, Inc., Santa Clara, CA, USA). Quantities of 100 μL of standard diluent and 100 μL of AH diluent were added to 96-well microplates coated with an antibody against WIF-1 or DKK-3, and subsequent procedures were performed according to the manufacturer's protocol. Color intensity was determined with a microplate reader (Molecular Devices, Sunnyvale, CA, USA). Duplicate samples were used in all assays.

Patient Data

Baseline data (pre-IVR) were obtained for the 62 nAMD patients whose AHs were analyzed by ELISA, including their age and sex, the presence of diabetes or controlled systemic hypertension, cigarette smoking status, the best corrected visual acuity (VA, logMAR), and fluorescein angiography (FA), indocyanine green angiography (ICGA), and SD-OCT results. A follow-up examination, including the VA, FA, and SD-OCT, was performed 1 month after three consecutive IVRs (post-IVR) instead of 1 month after two consecutive IVRs, as was the case during the collection of AH samples.

Neovascularization was subdivided into three categories according to previous descriptions.[6,25] Briefly, in type 1 NV, new vessels are located beneath the RPE. The type 1 NV patient group included 13 patients with polypoidal choroidal vasculopathy (PCV), which was diagnosed based on the presence of prominent "polyps" and a branching of the choroidal vascular network that was visualized by ICGA. In type 2 NV, new vessels have penetrated the RPE layer and are localized in the subretinal space. Type 3 NV, retinal angiomatous proliferation (RAP), was defined as the intraretinal proliferation of new vessels, which may originate from both retinal and choroidal circulation.[25–27] The presence of a retinal-choroidal anastomosis was identified with ICGA, and intraretinal hemorrhages and cystoid macular edema were also found in type 3 NV.

A 9 × 6-mm area of the macular region centered on the fovea was examined using SD-OCT (Spectralis HRA+OCT; Heidelberg Engineering, Heidelberg, Germany). In total, 25 volume scans (each with a length of 240 μm) were centered on the fovea, with an average of nine replicates of the B-scan image of each section. The eye-tracking system of the device was used to ensure that the scanning was performed in the correct position. For high-quality images, only images with a quality score greater than 16 dB were selected. The SD-OCT image from the horizontal scans of the midline was reviewed for the measurement of foveal microstructures by two retina specialists who were blinded to the VA and expression analysis results of the patients. The integrity of the foveal photoreceptor layer was evaluated using SD-OCT images of the external limiting membrane (ELM) and the inner and outer segment of the photoreceptor junction (IS/OS) within a 6000-μm diameter centered on the fovea. Manual measurement of the disrupted length of the ELM and IS/OS and of the thickness of the outer nuclear layer (ONL) was performed pre- and post-IVR using a caliper built into the software of the SD-OCT machine. A disruption in the ELM and IS/OS was defined as the loss of the hyperreflective line. The dim line was considered "visible" if it was detectable. The thickness of the ONL was defined as the distance between the internal limiting membrane and the ELM at the center of the fovea. If there was an absence or disruption of the ELM, the next visible reflective line was considered as the outer border of the ONL. The central macular thickness (CMT) was automatically calculated as the average retinal thickness within a circle with a 1000-μm diameter centered on the fovea (the center circle of the Early Treatment Diabetic Retinopathy Study grid) (software version 5.1.2.0; Heidelberg Engineering).

The choroidal images were obtained using enhanced-depth imaging OCT in SD-OCT. Seven sections encompassing the fovea were analyzed (100 averaged scans each). The choroidal thickness (ChT) was measured under the foveal center, vertically from the outer border of the hyperreflective line of the RPE to the inner border of the sclera.

Two measurements performed by two people were averaged. The intraclass correlation coefficients (ICCs) of the measured disrupted length of the ELM and those of the IS/OS and ONL thickness were 0.75, 0.82, and 0.70, respectively. The ICC of the measured ChT was 0.71.

Treatment response to IVR after three monthly IVRs was defined as follows: "no fluid" was defined as the presence of a "dry" macula that was lacking any retinal (intra- or subretinal) fluid as detected by SD-OCT, "less fluid" was defined as the decrease in but not the complete resolution of retinal fluid, and "fluid" was defined as minimal changes of retinal fluid.

Table 2. Changes in Clinical Parameters on SD-OCT and Wnt Modulators in 62 nAMD Patients Pre- and Post-IVR

	Pre-IVR, $n = 62$	Post-IVR, $n = 62$	*P* Value*
CMT, μm (SD)	449 (170)	302 (94)	<0.0001
Disrupted length of IS/OS, μm (SD)	2526 (1761)	1900 (1701)	0.0018
Disrupted length of ELM, μm (SD)	1615 (1691)	1056 (1379)	0.0008
ONL thickness, μm (SD)	100 (121)	76 (31)	0.1252
ChT, μm (SD)	227 (99)	206 (93)	<0.0001
LogMAR (SD)	0.68 (0.50)	0.53 (0.39)	0.0005
WIF-1, ng/mL (SD)	54.7 (31.0)	46.8 (31.4)	0.3535
DKK-3, ng/mL (SD)	114.3 (46.8)	111.9 (47.5)	0.5905

CMT, central macular thickness; IS/OS, junction between inner and outer segment of the photoreceptor; ELM, external limiting membrane; ONL, outer nuclear layer; ChT, choroidal thickness; LogMAR, logarithm of the minimum angle of resolution.

* Paired *t*-test.

Statistical Analysis

The statistical analysis was performed using SPSS version17.0 for Windows software (SPSS, Inc., Chicago, IL, USA). All values are presented as the means ± SDs. Bivariate relationships were analyzed using the Pearson correlation coefficient. The Kruskal-Wallis test and a post hoc multiple comparison test were performed to examine the differences in the values of WIF-1 and DKK-3 between different patient groups. A multivariate analysis was performed using multiple linear regression of the specific variables. The Mann-Whitney test was used to compare discrete variables between groups; *P* values less than 0.05 were considered statistically significant.

Results

Study Group

The AH of 74 patients with nAMD was acquired pre- and post-IVR for Western blot analysis (12 sets for discovery) and ELISA (62 sets for validation). For quantification and correlation analysis, only data from the validation set were used. Patient ages ranged from 57 to 84 years (average 71.2 ± 7.0 years). The baseline characteristics of the 62 AMD patients (whose AH

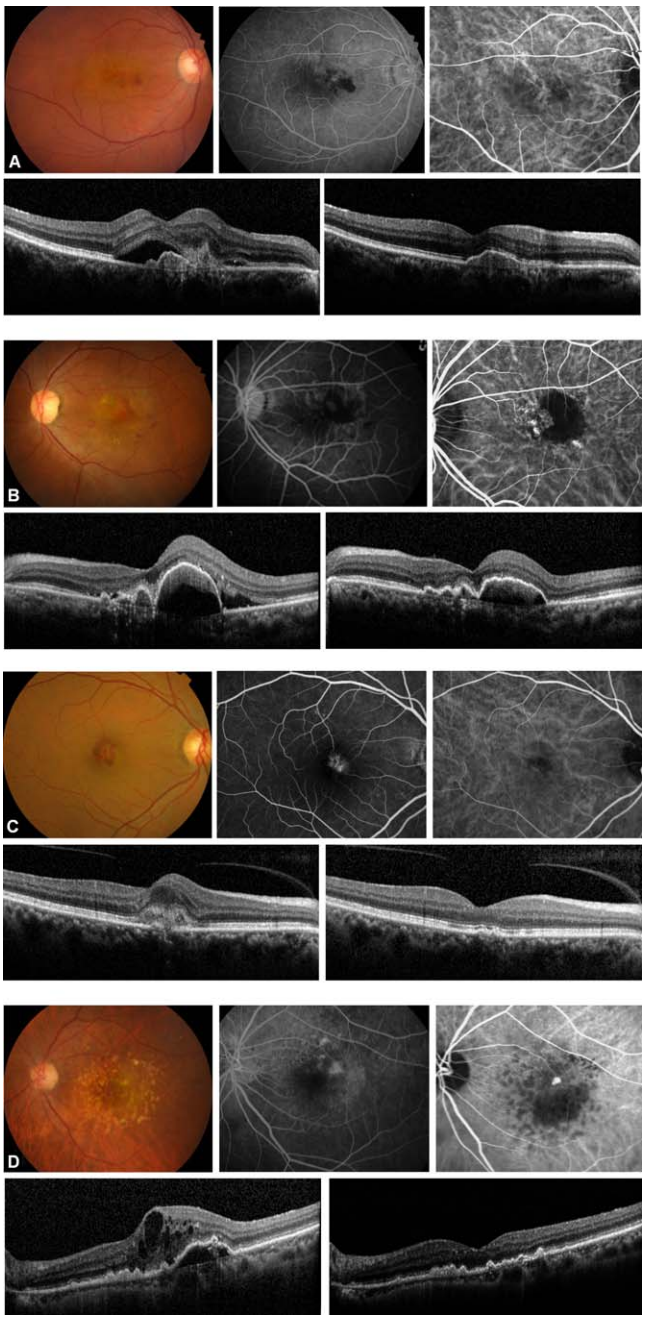

FIGURE 1. Color fundus photograph (*upper left*), FA (*upper middle*), ICGA (*upper right*), SD-OCT image before treatment (*lower left*), and SD-OCT image after treatment with ranibizumab (*lower right*) in nAMD patients. (**A**) A 74-year-old man with type 1 NV. His best-corrected visual acuity (BCVA) was 20/30, and the WIF-1 level was 29.2 ng/mL. Three months after IVR, intra- and subretinal fluid resolved, and BCVA improved to 20/25. Intact external limiting membrane (ELM) and the junction between the inner and outer segment of the photoreceptor (IS/OS) on SD-OCT were observed. (**B**) A 70-year-old woman with PCV. Polypoidal lesions were detected with ICGA. The BCVA was 20/40, and her WIF-1 level was 67.1 ng/mL. Three months after IVR, subretinal fluid resolved, with a persistent large defect in ELM and IS/OS on SD-OCT. The BCVA decreased to 20/150. (**C**) A 58-year-old woman with type 2 NV. The BCVA was 20/50, and her WIF-1 level was 12.3 ng/mL. Three months after IVR, intraretinal fluid and choroidal neovascularization resolved. The BCVA improved to 20/20. Intact ELM and IS/OS on SD-OCT were found. (**D**) A 77-year-old woman with type 3 NV. The ICGA showed retinal-choroidal anastomosis. The BCVA was 20/60, and her WIF-1 level was 125.0 ng/mL. Although cystoid edema, serous pigment epithelial detachment, and intraretinal retinal angiomatous proliferation lesions resolved 3 months after IVR, persistent large defects in the ELM and IS/OS were found on SD-OCT. The BCVA was 20/40.

pre- and post-IVR was analyzed by ELISA) are listed in Table 1. The type of NV was classified based on FA, ICGA, and SD-OCT findings in the baseline examination, as described in the Methods section. Forty-one eyes exhibited type 1 NV, 13 of which were diagnosed with PCV, 10 eyes exhibited type 2 NV, and 11 eyes exhibited type 3 NV.

The clinical data were obtained pre- and post-IVR (Table 2). The mean CMT of these 62 eyes decreased from a pre-IVR value of 449 μm (SD 170) to 302 μm (SD 94) post-IVR. A complete ELM was observed in 13 eyes, whereas a complete IS/OS was observed in 4 eyes, pre-IVR. Post-IVR, a complete ELM was observed in 19 eyes and a complete IS/OS was observed in 10 eyes. The mean disrupted length of the ELM of 62 eyes changed from 1615 μm (SD 1691) pre-IVR to 1056 μm (SD 1379) post-IVR. The mean disrupted length of the IS/OS of 62 eyes changed from 2526 μm (SD 1761) pre-IVR to 1900 μm (SD 1701) post-IVR. The mean ChT of these 62 eyes decreased from a pre-IVR value of 227 μm (SD 99) to 206 μm (SD 93) post-IVR. Regarding the response to treatment, 27 eyes (13 type 1, 9 type 2, and 5 type 3 NV) exhibited complete resolution of any retinal fluid post-IVR ("no fluid"), 29 eyes (21 type 1, 2 type 2, and 6 type 3) showed "less fluid," and 6 (all type 1) eyes showed "wet" macula ("fluid").

The mean Snellen VA was 20/100 pre-IVR and 20/60 post-IVR. The VA post-IVR improved in patients with type 1 or 2 NV; however, in patients with type 3 NV, VA was unchanged post-IVR, and the differences in VA among the three groups were not statistically significant ($P = 0.0530$ by ANOVA and $P = 0.0568$ by the Kruskal-Wallis test).

The CMT, disrupted lengths of the ELM and IS/OS, and ChT pre- and post-IVR were all associated with VA post-IVR (univariate analysis). The post-IVR VA was associated with the pre-IVR VA and pre-IVR CMT according to the multiple linear regression adjusted for age, sex, and the presence of diabetes or systemic hypertension ($R^2 = 0.8432$). A color fundus photograph, FA and ICGA results, SD-OCT image pre-IVR, and SD-OCT image post-IVR representative of nAMD patients are shown in Figure 1 and Supplementary Figure S1.

Western Blot Analysis and ELISA Measurement of Wnt Modulators

To confirm the expression of the Wnt modulators WIF-1 and DKK-3, which were found in the AH of nAMD patients by proteomic analysis in our previous study,[13,14] Western blot analyses of these proteins were performed. Equivalent amounts of proteins from the AHs of 12 nAMD patients pre- and post-IVR and their age- and sex-matched controls were loaded on the same gel. A profoundly increased expression of WIF-1 was detected in all 12 nAMD patients compared with their controls (Fig. 2). The level of DKK-3 also was increased in most patients compared with their controls.

Next, for the validation and quantitative measurement of the increased WIF-1 and DKK-3 levels in the AH of nAMD patients, ELISA analysis was performed on the 62 sets of AH samples. ELISA analysis demonstrated that WIF-1 (pre) and DKK-3 (pre) were elevated in 62 nAMD patients compared with the controls (54.7 vs. 23.0 ng/mL, $P < 0.0001$ for WIF-1; 114.3 vs. 93.0 ng/mL, $P = 0.0008$ for DKK-3, Student's *t*-test) (Table 1 and Fig. 3). WIF-1 (post) and DKK-3 (post) were also elevated in 62 nAMD patients compared with the controls (46.8 vs. 23.0 ng/mL, $P < 0.0001$ for WIF-1; 111.9 vs. 93.0 ng/mL, $P = 0.0002$ for DKK-3, Student's *t*-test). There

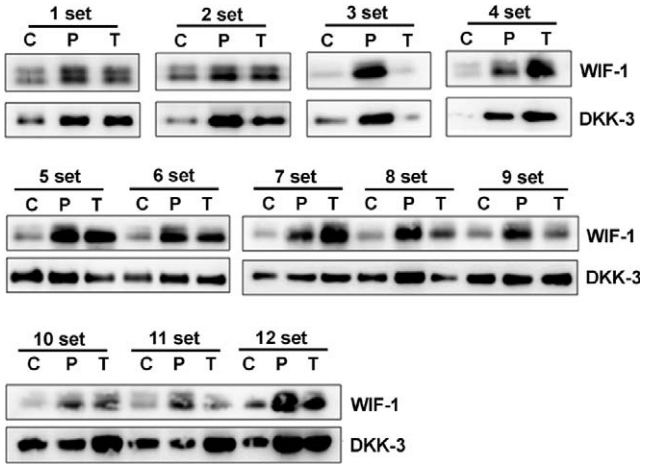

FIGURE 2. Western blot analysis of WIF-1 and DKK-3 in 12 nAMD patients before (P) and after (T) treatment with ranibizumab and in 12 matched control subjects (C).

were minor alterations in AH concentrations pre- and post-IVR ($P = 0.3535$ for WIF-1 and $P = 0.5905$ for DKK-3; paired *t*-test) (Table 2). WIF-1 (pre) and DKK-3 (pre) were positively correlated (Pearson correlation coefficient 0.5072, $P = 0.0002$); WIF-1 (post) and DKK-3 (post) were also well correlated (Pearson correlation coefficient 0.4529, $P = 0.0011$).

TABLE 3. SD-OCT Parameters, NV Type, and Vision According to the Levels of WIF-1 (Pre) in 62 nAMD Patients (Univariate Analysis)

	Univariate Analysis		
Variables	**Estimate**	**SE**	***P* Value**
WIF-1 (post)	0.5569	0.0815	<0.0001*
CMT (pre)	0.0233	0.0234	0.3235
CMT (post)	0.0913	0.0362	0.0149*
Disrupted length of IS/OS (pre)	0.0083	0.0020	0.0001*
Disrupted length of IS/OS (post)	0.0071	0.0019	0.0006*
Disrupted length of ELM (pre)	0.0033	0.0024	0.1625
Disrupted length of ELM (post)	0.0045	0.0026	0.0884
ONL (pre)	0.0242	0.0273	0.3795
ONL (post)	0.1274	0.1088	0.2473
ChT (pre)	−0.0054	0.0316	0.8657
ChT (post)	−0.0021	0.0333	0.9492
NV type			
1	−42.201	8.968	<0.0001*
2	−49.291	11.540	0.0001*
3	reference		
logMAR (pre)	3.6484	7.9960	0.6498
logMAR (post)	5.9446	8.9991	0.5114

SE, standard error; WIF-1 (post), level of WIF-1 one month after two consecutive intravitreal injections of ranibizumab.

* $P < 0.05$.

Association of Wnt Modulators With Clinical Parameters

The association of clinical variables, including SD-OCT and vision parameters, with the risk of high WIF-1 and DKK-3 levels in the AH of nAMD patients was analyzed.

Wnt Modulators Versus Retina Microstructure and Choroidal Thickness. High WIF-1 (pre) levels were associated with CMT (post), a disrupted length of IS/OS (pre), a disrupted length of IS/OS (post), and the type of NV (Table 3, Fig. 1, and Supplementary Fig. S1), whereas high WIF-1 (post) levels were associated with CMT (post). High DKK-3 (pre) levels were associated with a disrupted length of IS/OS (pre) in the univariate analysis. There was no association between the Wnt modulators and ChT. The final multivariate analysis of SD-OCT parameters in the prediction of high WIF-1 (pre) levels using multiple linear regression, adjusted for age, sex, and the presence of diabetes or systemic hypertension, showed that high WIF-1 (pre) levels were associated with a disrupted length of IS/OS (pre), a disrupted length of IS/OS (post), and high WIF-1 (post) levels, with a mean increase in WIF-1 (pre) of 0.44 ng/mL for every 100-μm increase in the disruption of IS/OS (pre) and a mean increase in WIF-1 (pre) of 0.47 ng/mL for every 100-μm increase in the disruption of IS/OS (post) (Table 4 and Fig. 4). Multivariate analysis of SD-OCT parameters associated with the prediction of high DKK-3 (pre) levels, adjusted for age, sex, and the presence of diabetes or systemic hypertension, showed that a high DKK-3 level was associated with the disruption of IS/OS (pre) and a high DKK-3 (post) level. These data suggest that patients who have high WIF-1 and DKK-3 protein levels have a stronger damage response,

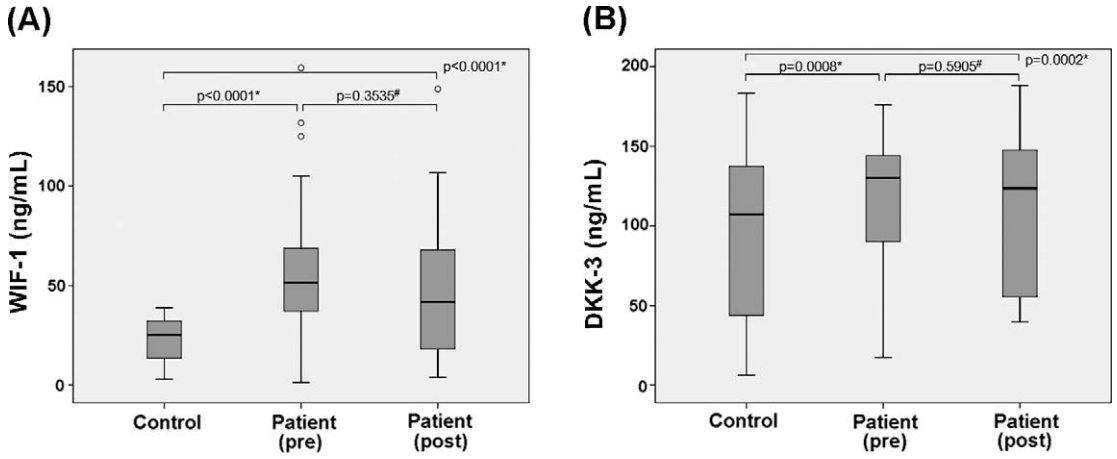

FIGURE 3. Aqueous levels of Wnt modulators ([**A**] the level of WIF-1 before treatment; [**B**] the level of DKK-3 before treatment) in 62 nAMD patients compared with 62 controls. The data are presented using box and whisker diagrams, with the median (first and third quartiles) in the box and the whiskers representing the minima and maxima of all data. pre, before treatment; post, after treatment. *P = Student's *t*-test; #P = paired *t*-test.

Table 4. Disrupted Length of IS/OS and NV Type According to the Levels of WIF-1 (Pre) in 62 nAMD Patients (Multivariate Analysis)

	Multivariate Analysis I			Multivariate Analysis II			Multivariate Analysis III		
Variables	Estimate	SE	*P* Value	Estimate	SE	*P* Value	Estimate	SE	*P* Value
WIF-1 (post)	0.5154	0.0798	<0.0001*	0.5313	0.0793	<0.0001*			
Disrupted length of IS/OS (pre)	0.0044	0.0015	0.0051*				0.0068	0.0020	0.0012*
Disrupted length of IS/OS (post)				0.0047	0.0015	0.0035*			
NV type									
1							−36.544	9.061	0.0002*
2							−38.833	12.183	0.0024*
3							reference		

Multivariate analysis I = explanatory variables were WIF-1 (post) and the disrupted length of IS/OS (pre), adjusted for age, sex, and the presence of diabetes or hypertension (adjusted R^2: 0.5393); Multivariate analysis II = explanatory variables were WIF-1 (post) and the disrupted length of IS/OS (post), adjusted for age, sex, and the presence of diabetes or hypertension (adjusted R^2: 0.5592); Multivariate analysis III = explanatory variables were the disrupted length of IS/OS (pre) and NV type, adjusted for age, sex, and the presence of diabetes or hypertension; adjusted R^2: 0.3674.

* $P < 0.05$.

which is manifested by the substantial disorganization of the photoreceptors and is observed as the disruption of IS/OS.

Wnt Modulators Versus Phenotypes of nAMD. Interestingly, the level of WIF-1 (pre) was significantly different among the three NV types (48.3 ± 22.5 for type 1, 41.3 ± 28.8 for type 2, and 90.5 ± 36.7 ng/mL for type 3, $P < 0.0001$ by ANOVA and $P = 0.0019$ by the Kruskal-Wallis test). A post hoc multiple comparison test confirmed that WIF-1 (pre) was significantly higher in type 3 NV patients than in type 1 or 2 patients (Fig. 5). Among the type 1 NV patients, there was no difference between sub-RPE CNV and PCV in the WIF-1 (pre) level (47.8 ± 20.8 for sub-RPE CNV, 49.4 ± 26.7 ng/mL for PCV, $P = 0.7157$; Mann-Whitney U test). When we analyzed the three NV groups using ANOVA or the Kruskal-Wallis test, no variables other than the WIF-1 (pre) level and ChT pre- and post-IVR were different; the value of CMT, the disrupted length of ELM, the disrupted length of IS/OS, and the logMAR pre- and post-IVR were not different among the groups, suggesting that none of the above SD-OCT or vision parameters influenced the finding that the WIF-1 (pre) level was highest in type 3 NV. However, the ChT pre- and post-IVR was different among the groups; ChT pre- and post-IVR was significantly lower in patients with type 3 NV (154 and 141 μm) than in those with type 1 or 2 NV (240 and 217 μm in type 1 NV; 265 and 243 μm in type 2 NV). However, the ChT pre- and post-IVR was not associated with WIF-1 (pre) in the univariate analysis. Multivariate analysis of ChT and NV type for the prediction of WIF-1 (pre) indicated that the effect of ChT pre- or post-IVR on the high WIF-1 (pre) level in type 3 NV was not significant (Table 5). Thus, the presence of RAP (type 3 NV) was associated with a greater probability of a high WIF-1 (pre) level, independent of ChT pre- and post-IVR, suggesting that a high WIF-1 level in the AH of nAMD patients may reflect profound photoreceptor damage, especially in patients with type 3 NV (Fig. 1D, Supplementary Fig. S1D).

Wnt Modulators Versus Response to Treatment and Vision. With respect to the response to treatment, the WIF-1 (pre) levels in 27 eyes exhibiting complete resolution of fluid ("no fluid") were lower (49.1 ng/mL) than those of 35 eyes with incomplete or little decrease in fluid (59.0 ng/mL), although this difference was not statistically significant (Mann-Whitney U test, $P = 0.0695$). The association between WIF-1 and VA pre- and post-IVR was not statistically significant.

Discussion

In the present study, we demonstrated for the first time that the levels of WIF-1 and DKK-3 were significantly elevated in the AH of patients with nAMD compared with those of control subjects. The association of these aqueous proteins with the

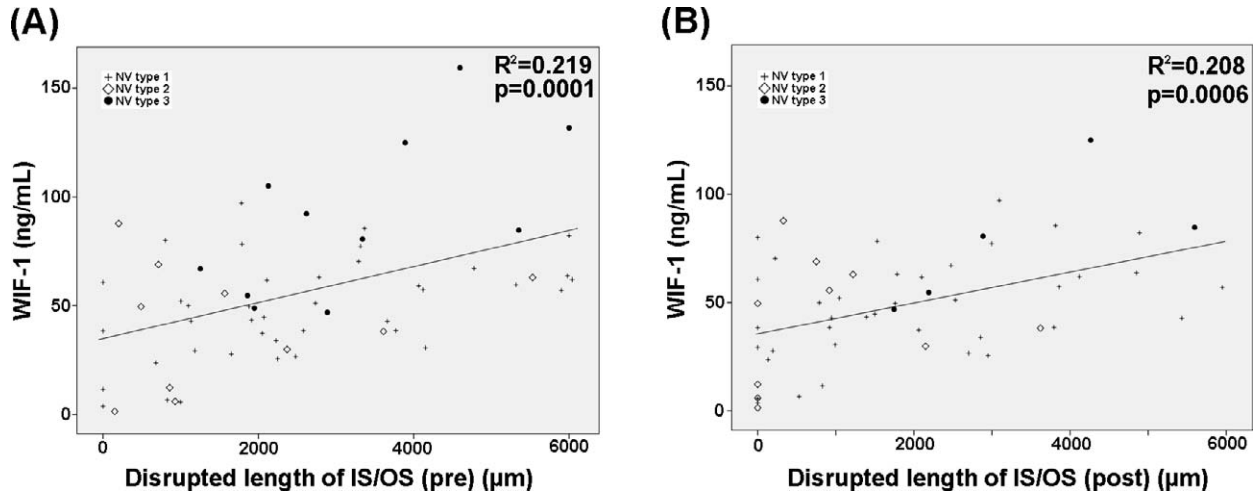

Figure 4. Association between WIF-1 before treatment (pre) and the IS/OS according to SD-OCT before and after treatment (pre (**A**) and post (**B**), respectively). A linear regression analysis shows that WIF-1 (pre) is significantly associated with the disrupted length of IS/OS pre and post ($R^2 = 0.219$, $P = 0.0001$ for IS/OS pre; $R^2 = 0.208$, $P = 0.0006$ for IS/OS post).

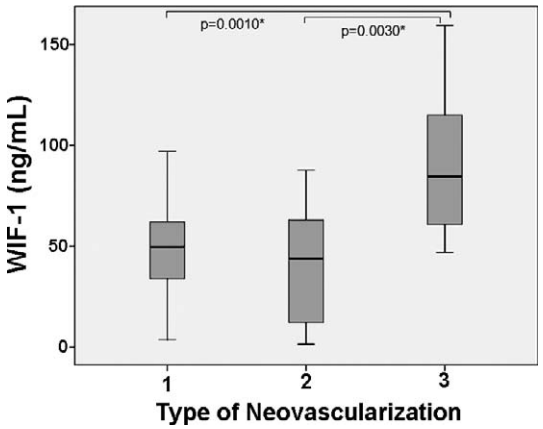

FIGURE 5. Association between the level of WIF-1 (pre) and the type of NV (1, 2, and 3). WIF-1 levels are significantly higher in type 3 NV patients than in type 1 or 2 NV patients (90.5 ± 36.7 ng/mL in type 3 vs. 48.3 ± 22.5 ng/mL in type 1 and 41.3 ± 28.8 ng/mL in type 2). *P values in the figure are derived from the Kruskal-Wallis test, and the P values derived from ANOVA are <0.0001 and 0.0002, respectively.

AMD phenotype has not been previously investigated. The present study evaluated the association of WIF-1 and DKK-3 with the severity of retinal damage and NV type. Multivariate analysis showed that the disruption of IS/OS (pre) and the disruption of IS/OS (post) had strong dependent associations with high WIF-1 (pre) levels, despite the general difficulty of validating clinical correlations for biological markers.[24] These findings provide evidence for an association of retinal damage with an increase in WIF-1 levels and demonstrate that WIF-1 may be an appropriate biomarker of retinal damage response in AMD.

Although the roles of Wnt signaling in the development of the retina, including stabilization of the rod photoreceptor synapse, have been more extensively described, its roles in later stages of retinal development and in the homeostasis and/or function of the adult retina also have been documented.[28] In addition, highly activated Wnt signaling in the ciliary margin and the ciliary epithelium of newborn murine eyes was dramatically attenuated in adult murine eyes, as the retina is the primary site of Wnt signaling in adult murine eyes.[29] Considering its putative role in antagonizing Wnt activity, WIF-1 should be expressed predominantly in the retina and concentrated in the photoreceptors and outer plexiform layer, with reduced expression in the inner nuclear layer and ganglion cell layer.[19] We also confirmed the increased expression of WIF-1 in the retinas of 10-week-old C57BL/6 mice exposed to bright light, whereas WIF-1 expression in the RPE was almost negligible (Supplementary Fig. S2). We speculate that in nAMD, Wnt signaling is increased in response to the retinal injury and is coordinated with the increased secretion of WIF-1 and DKK-3 (i.e., the levels of WIF-1 and DKK-3 in the AH reflect the degree of Wnt activation in the retina). The WIF-1 level in the plasma of patients with nAMD or controls appears to be negligible because we could not detect its expression by Western blot analysis (data not shown). Thus, the retina may be a major source of the increased WIF-1 in the AH of nAMD patients. A known target gene of Wnt activation is VEGF.[30] Although the exact mechanism of the regulation of Wnt signaling, including regulation by Wnt modulators, on anti-VEGF treatment in nAMD requires further investigation; the fact that the levels of Wnt modulators decreased after two consecutive IVRs in this study suggests that anti-VEGF therapy may cause some alterations of the intraocular environment that affect the levels of Wnt modulators. Thus, the levels of WIF-1 and DKK-3, which indicate the level of Wnt activation, could reflect the severity of AMD.

Retinal angiomatous proliferation, now described as type 3 NV,[26,27] represents approximately 10% to 20% of all cases of nAMD.[31,32] In the present study, 17.7% (11 of 62) of eyes exhibited type 3 NV. Retinal angiomatous proliferation has been reported to follow a more aggressive natural course than type 1 or 2 NV, despite the excellent response to anti-VEGF therapy with a dramatic reduction in CMT and intraretinal edema.[32,33] The occurrence of high rates of RPE atrophy at presentation and the development of new atrophy or geographic atrophy during follow-up have also been described.[32,34] Intriguingly, the WIF-1 level was by far the highest in patients with type 3 NV in this study. This result may suggest that the retina is markedly damaged during the course of RAP; this assertion is supported by the disrupted IS/OS on SD-OCT, which indicates that the retina and, particularly, the photoreceptors are damaged. A thin choroid and the possibly reduced choroidal perfusion in the macula also may contribute to a generally unfavorable visual recovery or functional gain[35]; however, the thin choroid of the patients with RAP in this study did not appear to influence the WIF-1 level. Additionally, this finding reinforces the notion that WIF-1 reflects the damage status of the retina, especially the photoreceptors.

The current study has several limitations. First, although we took into account several SD-OCT parameters, including CMT, IS/OS, ELM, ONL thickness, and ChT, as well as the type of NV, in the analysis of their association with Wnt modulators, we did not consider all the various phenotypes of AMD; for example, the type (drusenoid, serous, or fibrovascular) and size of pigment epithelial detachment, the size of NV, the type

TABLE 5. Choroidal Thickness and NV Type According to the Levels of WIF-1 (Pre) in 62 nAMD Patients (Multivariate Analysis)

	Multivariate Analysis I			Multivariate Analysis II		
Variables	**Estimate**	**SE**	***P* Value**	**Estimate**	**SE**	***P* Value**
WIF-1 (post)	0.5559	0.0863	<0.0001*	0.5541	0.0864	<0.0001*
ChT (pre)	0.0028	0.0313	0.9282			
ChT (post)				0.0076	0.0328	0.8189
NV Type						
1	−1.6196	9.5405	0.0972	−1.6433	9.529	0.0922
2	−2.4602	11.507	0.0385*	−2.4829	11.521	0.0371*
3	reference			reference		

Multivariate analysis I = explanatory variables were WIF-1 (post), ChT (pre), and NV type, adjusted for age, sex, and the presence of diabetes or hypertension; Multivariate analysis II = explanatory variables were WIF-1 (post), ChT (post), and NV type, adjusted for age, sex, and the presence of diabetes or hypertension.

* $P < 0.05$.

of polyp in PCV, or combined retinal hemorrhage. Because the eyes with large subretinal or intraretinal hemorrhage were excluded and WIF-1 is considered to be secreted in the retina and reflect the pathology of the retina in AMD, the influences of the above unconsidered parameters on the Wnt modulators in this study are not likely to be significant. Second, the disrupted length of the IS/OS or ELM line might have been overestimated due to the still-insufficient resolution of the SD-OCT device, the overlying pathological retina, or NV, especially before treatment, although only images of the IS/OS or ELM line with a quality score greater than 16 dB were selected for measurement.[36] However, reduced backscattering from the IS/OS, the ELM, and the other outer layers was not regarded as the result of disruption, but rather as the result of a shadowing effect. The dim IS/OS line was considered to be "visible" if it was still detectable; the loss of the hyperreflective line was regarded as "disruption" in the IS/OS. In addition, the assessment of IS/OS and ELM integrity after treatment was mostly done without difficulty because most nAMD eyes (56 among 62 patients) exhibited complete resolution or a decrease in retinal fluid or edema. Third, we did not find a significant association between VA and Wnt modulators in the present study, although the disruption of IS/OS was strongly associated with both vision and Wnt modulators.

This lack of significance may be attributed to the relatively small sample size from a heterogeneous patient population, the varied location of NV (sub- or juxta-foveal NV), or the different fixation points of these patients. However, we observed a trend toward an association between the response to treatment and the WIF-1 (pre) level. Further large-scale investigations may reveal the association of visual prognosis and Wnt modulators in the AH of patients with nAMD.

In conclusion, our results suggest that WIF-1 and DKK-3 levels are significantly elevated in the AH of nAMD patients and that their levels correlate with the severity of the outer retinal damage in nAMD. Our study, which demonstrated markedly elevated WIF-1 levels in the AH of patients with nAMD that were associated with the destructive response in the retina, also adds evidence of the involvement of Wnt signaling in the development and/or progression of AMD. Secreted WIF-1 in patients with nAMD could be a new AH biomarker with potential for the reflection of retinal status and, thus, the prediction of long-term prognosis. Further extended studies are needed to elucidate whether the modulation of WIF-1 could be a new approach for decreasing or preventing outer retinal damage in AMD.

Acknowledgments

Supported by the National Research Foundation of Korea funded by the Ministry of Science, ICT, and Future Planning (NRF-2012M3A9B2028333 and NRF-2012R1A1A11012171). The authors alone are responsible for the content and writing of the paper.

Disclosure: **K.H. Park**, None; **A.J. Choi**, None; **J. Yoon**, None; **D. Lim**, None; **S.J. Woo**, None; **S.J. Park**, None; **H.C. Kim**, None; **H. Chung**, None

References

1. Fritsche LG, Chen W, Schu M, et al. Seven new loci associated with age-related macular degeneration. *Nat Genet*. 2013;45:433–439, 439e1–439e2.
2. Churchill AJ, Carter JG, Lovell HC, et al. VEGF polymorphisms are associated with neovascular age-related macular degeneration. *Hum Mol Genet*. 2006;15:2955–2961.
3. Galan A, Ferlin A, Caretti L, et al. Association of age-related macular degeneration with polymorphisms in vascular endothelial growth factor and its receptor. *Ophthalmology*. 2010;117:1769–1774.
4. Seddon JM, Francis PJ, George S, et al. Association of CFH Y402H and LOC387715 A69S with progression of age-related macular degeneration. *JAMA*. 2007;297:1793–1800.
5. Funk M, Karl D, Georgopoulos M, et al. Neovascular age-related macular degeneration: intraocular cytokines and growth factors and the influence of therapy with ranibizumab. *Ophthalmology*. 2009;116:2393–2399.
6. dell'Omo R, Cassetta M, dell'Omo E, et al. Aqueous humor levels of vascular endothelial growth factor before and after intravitreal bevacizumab in type 3 versus type 1 and 2 neovascularization. A prospective, case-control study. *Am J Ophthalmol*. 2012;153:155–161.e2.
7. Yi H, Nakamura RE, Mohamed O, et al. Characterization of Wnt signaling during photoreceptor degeneration. *Invest Ophthalmol Vis Sci*. 2007;48:5733–5741.
8. Hu Y, Chen Y, Lin M, et al. Pathogenic role of the Wnt signaling pathway activation in laser-induced choroidal neovascularization. *Invest Ophthalmol Vis Sci*. 2013;54:141–154.
9. Chen Y, Hu Y, Moiseyev G, et al. Photoreceptor degeneration and retinal inflammation induced by very low-density lipoprotein receptor deficiency. *Microvasc Res*. 2009;78:119–127.
10. Osakada F, Ooto S, Akagi T, et al. Wnt signaling promotes regeneration in the retina of adult mammals. *J Neurosci*. 2007;27:4210–4219.
11. Xu Y, Gu Z, Shen B, et al. Roles of Wnt/beta-catenin signaling in retinal neuron-like differentiation of bone marrow mesenchymal stem cells from nonobese diabetic mice. *J Mol Neurosci*. 2013;49:250–261.
12. Nakamura RE, Hunter DD, Yi H, et al. Identification of two novel activities of the Wnt signaling regulator Dickkopf 3 and characterization of its expression in the mouse retina. *BMC Cell Biol*. 2007;8:52.
13. Kang GY, Bang JY, Choi AJ, et al. Exosomal proteins in the aqueous humor as novel biomarkers in patients with neovascular age-related macular degeneration. *J Proteome Res*. 2014;13:581–595.
14. Lee H, Choi AJ, Kang GY, et al. Increased 26S proteasome non-ATPase regulatory subunit 1 in the aqueous humor of patients with age-related macular degeneration. *BMB Rep*. 2014;47:292–297.
15. Leyns L, Bouwmeester T, Kim SH, et al. Frzb-1 is a secreted antagonist of Wnt signaling expressed in the Spemann organizer. *Cell*. 1997;88:747–756.
16. Glinka A, Wu W, Delius H, et al. Dickkopf-1 is a member of a new family of secreted proteins and functions in head induction. *Nature*. 1998;391:357–362.
17. Hsieh JC, Kodjabachian L, Rebbert ML, et al. A new secreted protein that binds to Wnt proteins and inhibits their activities. *Nature*. 1999;398:431–436.
18. Hackam AS, Strom R, Liu D, et al. Identification of gene expression changes associated with the progression of retinal degeneration in the rd1 mouse. *Invest Ophthalmol Vis Sci*. 2004;45:2929–2942.
19. Hunter DD, Zhang M, Ferguson JW, et al. The extracellular matrix component WIF-1 is expressed during, and can modulate, retinal development. *Mol Cell Neurosci*. 2004;27:477–488.
20. Mazieres J, He B, You L, et al. Wnt inhibitory factor-1 is silenced by promoter hypermethylation in human lung cancer. *Cancer Res*. 2004;64:4717–4720.
21. Ai L, Tao Q, Zhong S, et al. Inactivation of Wnt inhibitory factor-1 (WIF1) expression by epigenetic silencing is a common event in breast cancer. *Carcinogenesis*. 2006;27:1341–1348.

22. Kawakami K, Hirata H, Yamamura S, et al. Functional significance of Wnt inhibitory factor-1 gene in kidney cancer. *Cancer Res*. 2009;69:8603–8610.
23. Kansara M, Tsang M, Kodjabachian L, et al. Wnt inhibitory factor 1 is epigenetically silenced in human osteosarcoma, and targeted disruption accelerates osteosarcoma genesis in mice. *J Clin Invest*. 2009;119:837–851.
24. Hou HA, Kuo YY, Liu CY, et al. Distinct association between aberrant methylation of Wnt inhibitors and genetic alterations in acute myeloid leukaemia. *Br J Cancer*. 2011;105:1927–1933.
25. Freund KB, Zweifel SA, Engelbert M. Do we need a new classification for choroidal neovascularization in age-related macular degeneration? *Retina*. 2010;30:1333–1349.
26. Yannuzzi LA, Freund KB, Takahashi BS. Review of retinal angiomatous proliferation or type 3 neovascularization. *Retina*. 2008;28:375–384.
27. Freund KB, Ho IV, Barbazetto IA, et al. Type 3 neovascularization: the expanded spectrum of retinal angiomatous proliferation. *Retina*. 2008;28:201–211.
28. Liu H, Mohamed O, Dufort D, Wallace VA. Characterization of Wnt signaling components and activation of the Wnt canonical pathway in the murine retina. *Dev Dyn*. 2003;227:323–334.
29. Liu H, Thurig S, Mohamed O, et al. Mapping canonical Wnt signaling in the developing and adult retina. *Invest Ophthalmol Vis Sci*. 2006;47:5088–5097.
30. Easwaran V, Lee SH, Inge L, et al. beta-Catenin regulates vascular endothelial growth factor expression in colon cancer. *Cancer Res*. 2003;63:3145–3153.
31. Scott AW, Bressler SB. Retinal angiomatous proliferation or retinal anastomosis to the lesion. *Eye (Lond)*. 2010;24:491–496.
32. McBain VA, Kumari R, Townend J, Lois N. Geographic atrophy in retinal angiomatous proliferation. *Retina*. 2011;31:1043–1052.
33. Engelbert M, Zweifel SA, Freund KB. "Treat and extend" dosing of intravitreal antivascular endothelial growth factor therapy for type 3 neovascularization/retinal angiomatous proliferation. *Retina*. 2009;29:1424–1431.
34. Grunwald JE, Daniel E, Huang J, et al. Risk of geographic atrophy in the comparison of age-related macular degeneration treatments trials. *Ophthalmology*. 2014;121:150–161.
35. Yamazaki T, Koizumi H, Yamagishi T, Kinoshita S. Subfoveal choroidal thickness in retinal angiomatous proliferation. *Retina*. 2014;34:1316–1322.
36. Chung H, Park B, Shin HJ, Kim HC. Correlation of fundus autofluorescence with spectral-domain optical coherence tomography and vision in diabetic macular edema. *Ophthalmology*. 2012;119:1056–1065.

Investigative Ophthalmology & Visual Science